Adaptive Neural-Network Boundary Control for a Flexible Manipulator With Input Constraints and Model Uncertainties

Yong Ren, Zhijia Zhao, *Member, IEEE*, Chunliang Zhang, Qinmin Yang, *Senior Member, IEEE*, and Keum-Shik Hong, *Fellow, IEEE*

***Abstract*—This article develops an adaptive neural-network (NN) boundary control scheme for a flexible manipulator subject to input constraints, model uncertainties, and external disturbances. First, a radial basis function NN method is utilized to tackle the unknown input saturations, dead zones, and model uncertainties. Then, based on the backstepping approach, two adaptive NN boundary controllers with update laws are employed to stabilize the like-position loop subsystem and like-posture loop subsystem, respectively. With the introduced control laws, the uniform ultimate boundedness of the deflection and angle tracking errors for the flexible manipulator are guaranteed. Finally, the control performance of the developed control technique is examined by a numerical example.**

***Index Terms*—Adaptive neural network (NN) boundary control (BC), flexible manipulator, input constraints, model uncertainties.**

I. Introduction

THE FLEXIBLE manipulator is receiving increasing attention from many researchers due to its low weight, high flexibility, low energy consumption, and so on. However, the undesired vibration phenomenon in the flexible structure is often contradictory to the demand for the high-accuracy position [1], [2]. Thus, the vibration reduction for the flexible manipulator has aroused enormous excitement, and many good results have been achieved in the past decades [3]–[7]. The above-mentioned research achievements were mainly aimed at the discrete-infinite-dimensional dynamic model with some certain simplifications for flexibility, which may generate control spillover and destabilize the system. Therefore, effective control methods should be developed to resolve the above problems.

The flexible manipulator is described by a distributed parameter system (DPS). Boundary control (BC) is an effective strategy for stabilizing a DPS since fewer sensors and actuators are needed [8], [9]. In recent decades, a major advance has been made in the BC of DPSs. The BC has been employed to a variety of flexible structures, such as the flapping-wing micro aerial vehicle [10], [11]; the flexible hose [12], [13]; and the flexible string [14], [15]. In [16]–[18], the BC technique has been adopted to restrain the oscillation in a suspension cable system of a helicopter. The problem of uniform ultimate boundedness (UUB) has been investigated for an axially moving system in [19]–[21], where BC schemes have been constructed by using the Lyapunov criteria. In [22]–[24], the BC has been studied for flexible mechanical systems: with the proposed control technologies, the deflections have been pledged to be uniformly ultimately bounded.

Due to the universal approximation ability, the radial basis function neural-network (RBFNN) method is usually employed to approximate unknown functions [25]–[37]. A robust adaptive neural-network (NN) control law has been derived for a class of multiple-input–multiple-output systems in [38], where the NN technology has been utilized to approach an unknown gain function matrix. The problem of a dynamic surface control has been investigated for a class of uncertain strict-feedback nonlinear systems in [39], while the uncertain system function has been approximated by using RBFNN. For a teleoperation system, the stability has been analyzed in [40], where the RBFNN technique has been utilized to compensate for the effects caused by dynamics uncertainties and communication delays. For a class of time-varying-constrained nonlinear systems, the time-varying barrier Lyapunov functions has been employed in [41]–[43] to pledge that constraints are not violated, where NN has been used to approach the unknown intermediate control functions. For robotic manipulators [44]–[46], the problem of UUB has been addressed, where the NN strategy has

Manuscript received February 1, 2020; revised June 24, 2020; accepted August 21, 2020. Date of publication October 1, 2020; date of current version October 12, 2021. This work was supported in part by the National Natural Science Foundation of China under Grant 61803109, Grant 62003193, and Grant 51775122; in part by the Innovative School Project of Education Department of Guangdong under Grant 2017KQNCX153; in part by the Science and Technology Planning Project of Guangzhou City under Grant 201904010494; in part by the Scientific Research Projects of Guangzhou Education Bureau under Grant 202032793; and in part by the National Research Foundation (NRF) of Korea under the auspices of the Ministry of Science and ICT, Korea under Grant NRF-2020R1A2B5B03096000. This article was recommended by Associate Editor H. Qiao. *(Corresponding author: Zhijia Zhao.)*

Yong Ren is with the College of Electrical Engineering and Automation, Shandong University of Science and Technology, Qingdao 266590, China (e-mail: yren0511@126.com).

Zhijia Zhao and Chunliang Zhang are with the School of Mechanical and Electrical Engineering, Guangzhou University, Guangzhou 510006, China (e-mail: zhjzhaoscut@163.com; nhzcl@163.com).

Qinmin Yang is with the State Key Laboratory of Industrial Control Technology, College of Control Science and Engineering, Zhejiang University, Hangzhou 310027, China (e-mail: qmyang@zju.edu.cn).

Keum-Shik Hong is with the School of Mechanical Engineering, Pusan National University, Busan 46241, South Korea (e-mail: kshong@pusan.ac.kr).

Color versions of one or more figures in this article are available at https://doi.org/10.1109/TCYB.2020.3021069.

Digital Object Identifier 10.1109/TCYB.2020.3021069

been employed to approximate the unknown system function. According to the aforementioned articles, many excellent research results on tackling unknown system uncertainties or input constraints have been achieved by using the NN technique, but these research results were all related to ordinary differential equations. For the DPS described by partial differential equations, the technology of NN has been adopted to approximate unknown system dynamics [6], [47] and input constraints [48], [49]. However, the mixed effects of unknown input saturations, dead zones, model uncertainties, and boundary disturbances may enhance the difficulty of the controller design and stability analysis for the DPS. Although notable progress in NNs for DPSs has been achieved, no research has been reported on utilizing an NN technique to tackle the mixed problem of unknown input saturation, dead zone, and model uncertainties in flexible manipulator systems, which inspires our study.

In this article, we consider a flexible manipulator system with input constraints, model uncertainties, and external disturbances. The control design is divided into two parts: one is for the like-position loop subsystem and another is for the like-posture loop subsystem. By employing the Lyapunov principle, the adaptive NN BC (ANNBC) laws are introduced for the like-position loop subsystem and like-posture loop subsystem, respectively. The main contributions of this article are summarized as follows.

1) In contrast to [50], the endpoint payload in the flexible manipulator (i.e., one of the most important skills) is considered in this article.
2) In [51] and [52], the related parameters of input saturation and input dead zones are supposed to be known, which are difficult to obtain in many cases. Inspired by this point, the problem of unknown input saturations, input dead zones, and model uncertainties is addressed by using the ANNBC strategy and the backstepping technique in this article.
3) Based on the derived ANNBC laws, the deflection and the angular displacement tracking error in the flexible manipulator system can ultimately remain in a small compact set.

Notations: $\mathfrak{R}$ and $\mathfrak{R}^k$ present the real number and the set of k-dimensional vectors, respectively. tanh is the hyperbolic tangent function. A class-$\mathfrak{K}$ function $\beta(t) : [0, k) \to [0, \infty)$ with $\beta(0) = 0$ denotes that it is strictly increasing, where $k > 0$. $K(t) > 0$ illustrates that $K(t)$ is a positive-definite function. $\pi_1 >> \pi_2$ represents that π_1 is much bigger than π_2. $\min\{b_1, b_2, \ldots, b_n\}$ and $\max\{b_1, b_2, \ldots, b_n\}$ denote the minimum and maximum values between/among $b_1, b_2, \ldots, b_n$, respectively, $n \geq 2$. For $\forall a \in [0, r]$ and t belongs to $[0, \infty)$, the abbreviations of system variables are listed in Table I.

II. Problem Statement and Preliminaries

Fig. 1 shows a diagrammatic drawing for a flexible manipulator. The coordinate axis *YOZ* denotes the inertial coordinate system while the coordinate axis *yOz* represents the body-fixed coordinate system. The system parameters of the flexible manipulator are given in Table II.

TABLE I
ABBREVIATIONS OF SYSTEM VARIABLES

Symbol	Abbreviation	Symbol	Abbreviation
$\frac{\partial s(a,t)}{\partial t}$	$s_t(a,t)$	$\frac{\partial s(a,t)}{\partial a}$	$s_a(a,t)$
$\frac{\partial^2 s(a,t)}{\partial t^2}$	$s_{tt}(a,t)$	$\frac{\partial^2 s(a,t)}{\partial a^2}$	$s_{aa}(a,t)$
$\frac{\partial^2 s(a,t)}{\partial a \partial t}$	$s_{at}(a,t)$	$\frac{\partial^3 s(a,t)}{\partial a^3}$	$s_{aaa}(a,t)$
$\frac{\partial^3 s(a,t)}{\partial a^2 \partial t}$	$s_{aat}(a,t)$	$\frac{\partial w(a,t)}{\partial a}$	$w_a(a,t)$
$\frac{\partial^2 w(a,t)}{\partial a^2}$	$w_{aa}(a,t)$	$\frac{\partial^2 w(a,t)}{\partial a \partial t}$	$w_{at}(a,t)$
$\frac{\partial^3 w(a,t)}{\partial a^3}$	$w_{aaa}(a,t)$	$\frac{\partial^3 w(a,t)}{\partial a^2 \partial t}$	$w_{aat}(a,t)$
$\frac{\partial^4 w(a,t)}{\partial a^3 \partial t}$	$w_{aaat}(a,t)$	$\frac{\partial^4 w(a,t)}{\partial a^4}$	$w_{aaaa}(a,t)$

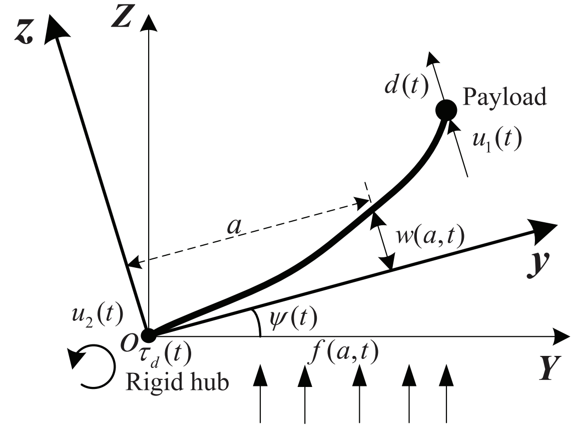

Fig. 1. Diagrammatic drawing for the flexible manipulator.

TABLE II
PARAMETERS OF FLEXIBLE MANIPULATOR

Symbol	Description
r	Length of the flexible manipulator
M_p	Mass of the payload
$s(a,t) = w(a,t) + a\psi(t)$	Displacement of the flexible manipulator in the coordinate axis YOZ
$w(a,t)$	Elastic deflection of the flexible manipulator in the coordinate axis yOz
$\psi(t)$	Angular displacement of the rigid hub
$f(a,t)$	Distributed disturbance
$u_1(t)$	Control force of the like-position loop
$d(t)$	Disturbance of the like-position loop
$u_2(t)$	Control torque of the like-posture loop
$\tau_d(t)$	Disturbance torque of the like-posture loop
μ	Uniform mass per unit length of the flexible manipulator
EI	Uniform flexural rigidity
I_m	Inertia moment of the rigid hub

According to [53], the system equations of a flexible manipulator with external disturbances and uncertainties can be represented as follows:

$$\mu s_{tt}(a,t) = -EIw_{aaaa}(a,t) + f(a,t), \text{ for } \forall a \in (0,r) \quad (1)$$

under the boundary conditions

$$M_p s_{tt}(r,t) = u_1(t) + d(t) + EIw_{aaa}(r,t) + \Delta f_1 \quad (2)$$

$$I_m \ddot{\psi}(t) = u_2(t) + \tau_d(t) + EIw_{aa}(0,t) + \Delta f_2 \quad (3)$$

$$w(0,t) = w_a(0,t) = w_{aa}(r,t) = 0 \quad (4)$$

where Δf_1 and Δf_2 denote the system uncertainties.

Due to the output limitation of the actuator, the phenomenon of input saturation exists in many mechanical equipment. Thus, input saturation is necessary to be considered for the flexible manipulator and can be described as follows:

$$\varpi_i = \mathrm{sat}(\kappa_i) = \begin{cases} \kappa_{Mi}, & \text{if } \kappa_i \geq \kappa_{Mi} \\ \kappa_i, & \text{if } \kappa_{mi} < \kappa_i < \kappa_{Mi} \\ \kappa_{mi}, & \text{if } \kappa_i \leq \kappa_{mi} \end{cases} \tag{5}$$

where $\kappa_{Mi} > 0$ and $\kappa_{mi} < 0$ are the unknown upper and lower saturation levels of the control κ_i, respectively, $i = 1,\ 2$.

Moreover, since the actuator output is insensitive to input in the particular area around zero, the phenomenon of dead zone is also considered for the flexible manipulator and presented by

$$\varrho_i = D(\varpi_i) = \begin{cases} k_{ri}(\varpi_i - m_{ri}), & \text{if } \varpi_i \geq m_{ri} \\ 0, & \text{if } m_{li} < \varpi_i < m_{ri} \\ k_{li}(\varpi_i - m_{li}), & \text{if } \varpi_i \leq m_{li} \end{cases} \tag{6}$$

with $m_{li} < 0$ and $m_{ri} > 0$ being the unknown dead-zone ranges, and $k_{li} > 0$ and $k_{ri} > 0$ being the unknown slope parameters.

Inspired by [54], let D^+ be the right inverse of D which satisfies $D \cdot D^+ = I$, then

$$\kappa_i = D^+(\nu_i) = \begin{cases} \nu_i/k_{ri} + m_{ri}, & \text{if } \nu_i > 0 \\ 0, & \text{if } \nu_i = 0 \\ \nu_i/k_{li} + m_{li}, & \text{if } \nu_i < 0 \end{cases} \tag{7}$$

with ν_i being the designed control input.

Thus, according to [54], the problem of input saturation and input dead zone can be transformed into a new input saturation problem, and the new input saturation can be described as follows:

$$u_i = D\big(\mathrm{sat}\big(D^+(\nu_i)\big)\big) = \begin{cases} k_{ri}(\kappa_{Mi} - m_{ri}) \\ \text{if } \nu_i \geq k_{ri}(\kappa_{Mi} - m_{ri}) \\ \nu_i, \quad \text{if } k_{li}(\kappa_{mi} - m_{li}) \\ < \nu_i < k_{ri}(\kappa_{Mi} - m_{ri}) \\ k_{li}(\kappa_{mi} - m_{li}) \\ \text{if } \nu_i \leq k_{li}(\kappa_{mi} - m_{li}). \end{cases} \tag{8}$$

Define $\Delta_i = \Delta f_i + \Delta u_i$ with $\Delta u_i = u_i - \nu_i$, then (2) and (3) can be changed as

$$M_p s_{tt}(r,t) = \nu_1(t) + \Delta_1 + d(t) + EIw_{aaa}(r,t) \tag{9}$$

$$I_m \ddot{\psi}(t) = \nu_2(t) + \Delta_2 + \tau_d(t) + EIw_{aa}(0,t). \tag{10}$$

Letting $z_1(t) = s(r,t)$, $z_2(t) = s_t(r,t)$, $z_3(t) = e_\psi(t) = \psi(t) - \psi_r$, and $z_4(t) = \dot{e}_\psi(t)$ with ψ_r denoting a constant reference signal of the angular displacement, (9) and (10) can be represented as

$$\dot{z}_1(t) = z_2(t) \tag{11}$$

$$\dot{z}_2(t) = \frac{1}{M_p}\{\nu_1(t) + \Delta_1 + d(t) + EIw_{aaa}(r,t)\} \tag{12}$$

$$\dot{z}_3(t) = z_4(t) \tag{13}$$

$$\dot{z}_4(t) = \frac{1}{I_m}\{\nu_2(t) + \Delta_2 + \tau_d(t) + EIw_{aa}(0,t)\}. \tag{14}$$

For the flexible manipulator system described by (1), (4), and (11)–(14), the control objectives are stated as follows.

1) To compensate for the effects of input constraints, model uncertainties, and external disturbances.
2) To suppress the vibration of the flexible manipulator.
3) To ensure that the angular displacement of the rigid hub $\psi(t)$ can track the desired trajectory ψ_r.

To realize the aforementioned control objectives for the flexible manipulator, the following assumptions and lemmas are needed.

Assumption 1 [50]: For the external disturbances $f(a,t)$, $d(t)$, and $\tau_d(t)$, the following conditions are satisfied:

$$|f(a,t)| \leq \delta_1, |d(t)| \leq \delta_2, |\tau_d(t)| \leq \delta_3 \quad \forall\ a \in (0,r)$$

with $\delta_1 > 0$, $\delta_2 > 0$, and $\delta_3 > 0$ being unknown constants.

In addition, for the system uncertainties Δf_1 and Δf_2, there exist unknown positive constants δ_4 and δ_5 such that $|\Delta f_1| \leq \delta_4$ and $|\Delta f_2| \leq \delta_5$.

Assumption 2: Although input saturations and input dead zones are considered in this article, there exist controllers such that the control targets can be achieved. Moreover, the absolute values of saturation levels are sufficiently larger than the absolute values of dead-zone ranges, respectively, that is, $|\kappa_{Mi}| >> |m_{ri}|$ and $|\kappa_{mi}| >> |m_{li}|$, $i = 1, 2$.

Lemma 1 [55]: For $\forall\ \xi_1(a,t), \xi_2(a,t) \in \Re$, it follows that:

$$\xi_1(a,t)\xi_2(a,t) \leq \epsilon_1 \xi_1^2(a,t) + \frac{1}{\epsilon_1}\xi_2^2(a,t)$$

with $\epsilon_1 > 0$ being a constant.

Moreover, for a first-order continuous differentiable function $\eta(a,t)$ with respect to a, under $\eta(0,t) = 0$ and $\eta_a(0,t) = 0$, the following inequalities hold:

$$\eta^2(a,t) \leq r\int_0^r \eta_a^2(a,t)da$$

$$\eta_a^2(a,t) \leq r\int_0^r \eta_{aa}^2(a,t)da.$$

Lemma 2 [55]: For $\forall\ \hbar(t) \in \Re$, the following inequality holds:

$$|\hbar(t)| - \hbar(t)\tanh\left(\frac{\hbar(t)}{\epsilon_2}\right) \leq 0.2785\epsilon_2$$

with $\epsilon_2 > 0$ being a constant.

Lemma 3 [38]: For the unknown continuous function $S(Z) : \Re^m \to \Re$, the method of the RBFNN is adopted to approximate it

$$S(Z) = \hat{W}^T \Upsilon(Z) + \varepsilon$$

with $Z = [z_1, z_2, \ldots, z_m]^T \in \Re^m$ being the input of NN, $\hat{W} \in \Re^n$ being the weight vector of NN, $\Upsilon(Z) = [\Upsilon_1(Z), \Upsilon_2(Z), \ldots, \Upsilon_n(Z)]^T \in \Re^n$ and ε being the basis function and the approximation error of NN, respectively. The optimal weight vector W^* can be described by

$$W^* = \arg\min_{\hat{W}\in\Pi_s}\left\{\sup_{Z\in\Pi_r}\left|\hat{S}\left(Z|\hat{W}\right) - S(Z)\right|\right\}$$

where $\Pi_s = \{\hat{W} | \|\hat{W}\| \leq K\}$ is a valid field of the vector with K being a design value, Π_r is an allowable set of the state vectors, and $\hat{S}(Z|\hat{W}) = \hat{W}^T\Upsilon(Z)$.

Then, with the optimal weight value, it has

$$S(Z) = W^{*T}\Upsilon(Z) + \varepsilon^*$$

where ε^* is the ideal approximation error satisfying $|\varepsilon^*| \le \bar{N}$, with $\bar{N}$ being an unknown positive constant.

Lemma 4 [56]: Assume that the first-order continuous differentiable function $H(\theta) > 0$ satisfies: 1) the initial value of $H(\theta)$ is bounded; 2) $\chi_1(\|\theta\|) \le H(\theta) \le \chi_2(\|\theta\|)$ with the functions $\chi_1(\|\theta\|)$ and $\chi_2(\|\theta\|)$ being class-$\mathfrak{K}$ functions; and 3) $\dot{H}(\theta) \le -\gamma_1 H(\theta) + \gamma_2$, with $\gamma_1 > 0$ and $\gamma_2 > 0$ being constants, then θ is uniformly bounded.

Remark 1: Since the coordinate axis yOz is chosen such that the axis Oy is tangent to the beam at the base, $\omega(0, t) = 0$ and $\omega_a(0, t) = 0$ hold. In addition, $\omega_{aa}(r, t) = 0$ means that the bending moment of the flexible manipulator at the endpoint $a = r$ is zero [57].

Remark 2: In this article, the controllability is assumed to be satisfied, that is, there exists a control scheme such that the proposed control problems can be solved. Thus, if the disturbances are unbounded, then the flexible manipulator system will be uncontrollable. Moreover, in practical engineering, since the energy of disturbance is bounded, Assumption 1 is reasonable.

Remark 3: In Assumption 2, if the absolute values of saturation levels are equal or less than the absolute values of dead-zone ranges, the outputs of actuators will be 0 which is in conflict with the controllability of the flexible manipulator. Hence, the absolute values of saturation levels need to be sufficiently larger than the absolute values of dead-zone ranges.

III. ANNBC Design and Convergence Analysis

In this section, the BC technology is adopted to investigate the convergence of the flexible manipulator system. By employing the backstepping strategy, the control design is divided into two parts: one part is developed for the like-position loop subsystem; and another part is constructed for the like-posture loop subsystem. Based on the proposed control laws, the UUB of the closed-loop system can be ensured for the flexible manipulator.

A. Like-Position Loop Control Design

The backstepping method is adopted to derive the control law for the like-position loop subsystem of the flexible manipulator. In the following contents, the control design process is described.

Step 1: First, the following definitions are given by:

$$\Phi_1(t) = z_1(t) \tag{15}$$

$$\Phi_2(t) = z_2(t) - \omega_1(t) = \dot{\Phi}_1(t) - \omega_1(t) \tag{16}$$

with $\omega_1(t)$ being a virtual control. The virtual control can be introduced by

$$\omega_1(t) = -h_1\Phi_1(t) - w_a(r, t) + w_{aaa}(r, t) \tag{17}$$

with $h_1 > 0$ representing a constant. The Lyapunov function $W_1(t)$ is constructed by

$$W_1(t) = \frac{1}{2}\Phi_1^2(t). \tag{18}$$

Invoking (16)–(18), the derivative of $W_1(t)$ can be calculated as

$$\begin{aligned}\dot{W}_1(t) &= \Phi_1(t)\dot{\Phi}_1(t)\\ &= \Phi_1(t)[\Phi_2(t) + \omega_1(t)]\\ &= -h_1\Phi_1^2(t) + \Phi_1(t)[-w_a(r, t) + w_{aaa}(r, t)]\\ &\quad + \Phi_1(t)\Phi_2(t).\end{aligned} \tag{19}$$

Step 2: Choose the Lyapunov function $W_2(t)$ as follows:

$$W_2(t) = W_1(t) + \frac{M_p}{2}\Phi_2^2(t). \tag{20}$$

Considering (12), (16), and (20), it has

$$\begin{aligned}\dot{W}_2(t) &= \dot{W}_1(t) + M_p\Phi_2(t)\dot{\Phi}_2(t)\\ &= -h_1\Phi_1^2(t) + \Phi_1(t)[-w_a(r, t) + w_{aaa}(r, t)]\\ &\quad +\Phi_1(t)\Phi_2(t) + \Phi_2(t)\\ &\quad \times \left[\nu_1(t) + \Delta_1 + d(t) + EIw_{aaa}(r, t) - M_p\dot{\omega}_1(t)\right].\end{aligned} \tag{21}$$

Thus, the like-position loop controller is developed as follows:

$$\begin{aligned}\nu_1(t) &= -h_2\Phi_2(t) - EIw_{aaa}(r, t) + M_p\dot{\omega}_1(t) - \Phi_1(t)\\ &\quad - d(t) - \Delta_1\end{aligned} \tag{22}$$

with $h_2 > 0$ being a constant.

However, $d(t)$ and Δ_1 are unknown, thus they cannot be applied to control design. To approximate the unknown variable Δ_1, the RBFNN is adopted due to its universal approximation ability. The unknown disturbance $d(t)$ can be tackled with the adaptive technology.

According to Lemma 3, the unknown function Δ_1 can be described by

$$\Delta_1 = U_1^{*T}\Sigma_1(X_1) + \varepsilon_1^* \tag{23}$$

with U_1^* and ε_1^*, respectively, being the unknown ideal weight vector and optimal approximation error, $\Sigma_1(X_1)$ being the basis function, and $X_1 = [\Phi_1(t), \Phi_2(t), \dot{\omega}_1(t), w_a(r, t), w_{aaa}(r, t)]$.

Since the ideal weight vector U_1^* is unknown, the updating law is developed as follows:

$$\dot{\hat{U}}_1(t) = -g_1\Big[g_2\hat{U}_1(t) - \Sigma_1(X_1)\Phi_2(t)\Big] \tag{24}$$

with $\hat{U}_1(t)$ being the estimation of the unknown constant U_1^*, $g_1 > 0$ and $g_2 > 0$ denoting constants.

In addition, from Lemma 3, there is an unknown constant $\bar{\varepsilon}_1^* > 0$ such that $|\varepsilon_1^*| \le \bar{\varepsilon}_1^*$. Furthermore, considering Assumption 1 and defining $D_{c1}(t) = d(t) + \varepsilon_1^*$, it derives that $|D_{c1}(t)| \le \bar{D}_{c1}$, where $\bar{D}_{c1}$ is an unknown constant.

Hence, an ANNBC law for the like-position loop subsystem of the flexible manipulator is designed as follows:

$$\dot{\hat{\bar{D}}}_{c1}(t) = -\zeta_1\zeta_2\hat{\bar{D}}_{c1} + \zeta_2\Phi_2(t)\tanh\left(\frac{\Phi_2(t)}{\varsigma_1}\right) \tag{25}$$

$$\dot{\hat{U}}_1(t) = -g_1\Big[g_2\hat{U}_1(t) - \Sigma_1(X_1)\Phi_2(t)\Big] \tag{26}$$

$$\begin{aligned}\nu_1(t) &= -h_2\Phi_2(t) - EIw_{aaa}(r, t) + M_p\dot{\omega}_1(t) - \Phi_1(t)\\ &\quad - \hat{\bar{D}}_{c1}(t)\tanh\left(\frac{\Phi_2(t)}{\varsigma_1}\right) - \hat{U}_1^T(t)\Sigma_1(X_1)\end{aligned} \tag{27}$$

with $\zeta_1 > 0$, $\zeta_2 > 0$, and $\varsigma_1 > 0$ being constants, and $\hat{\bar{D}}_{c1}(t)$ being the estimation of the unknown constant $\bar{D}_{c1}$.

Substituting (23) and (27) into (21), and invoking Lemma 2 and $|D_{c1}(t)| \leq \bar{D}_{c1}$, it derives

$$\begin{aligned}\dot{W}_2(t) \leq& -h_1\Phi_1^2(t) - h_2\Phi_2^2(t) + \tilde{\bar{D}}_{c1}(t)\Phi_2(t)\\ &\times \tanh\left(\frac{\Phi_2(t)}{\varsigma_1}\right) + \Phi_2(t)\tilde{U}_1^T(t)\Sigma_1(X_1) + \Phi_1(t)\\ &\times [-w_a(r,t) + w_{aaa}(r,t)] + 0.2785\varsigma_1\bar{D}_{c1} \quad (28)\end{aligned}$$

where $\tilde{U}_1(t) = U_1^* - \hat{U}_1(t)$ and $\tilde{\bar{D}}_{c1}(t) = \bar{D}_{c1} - \hat{\bar{D}}_{c1}(t)$.

Then, the Lyapunov function is constructed as follows:

$$W_O(t) = W_2(t) + \frac{1}{2g_1}\tilde{U}_1^T(t)\tilde{U}_1(t) + \frac{1}{2\zeta_2}\tilde{\bar{D}}_{c1}^2(t). \quad (29)$$

Invoking (25), (26), (28), (29), and Lemma 1, the derivative of $W_O(t)$ is described as follows:

$$\begin{aligned}\dot{W}_O(t) =& \dot{W}_2(t) + \frac{1}{g_1}\tilde{U}_1^T(t)\dot{\tilde{U}}_1(t) + \frac{1}{\zeta_2}\tilde{\bar{D}}_{c1}(t)\dot{\tilde{\bar{D}}}_{c1}(t)\\ \leq& -(h_1 - \pi_1 - \pi_2)\Phi_1^2(t) - h_2\Phi_2^2(t) - \frac{g_2}{2}\tilde{U}_1^T(t)\\ &\times \tilde{U}_1(t) - \zeta_1\left(1 - \frac{1}{\pi_3}\right)\tilde{\bar{D}}_{c1}^2(t) + \zeta_1\pi_3\bar{D}_{c1}^2\\ &+ \frac{r}{\pi_1}\int_0^r w_{aa}^2(a,t)da + \frac{1}{\pi_2}w_{aaa}^2(r,t)\\ &+ \frac{g_2}{2}U_1^{*T}U_1^* + 0.2785\varsigma_1\bar{D}_{c1} \quad (30)\end{aligned}$$

with $\pi_1 > 0$, $\pi_2 > 0$, and $\pi_3 > 0$ being constants.

B. Like-Posture Loop Control Design

In this section, the BC is investigated by employing the backstepping strategy for the like-posture loop subsystem of the flexible manipulator. The control design process is shown as follows.

Step 1: Define

$$\Phi_3(t) = z_3(t) \quad (31)$$

$$\Phi_4(t) = z_4(t) - \omega_2(t) = \dot{\Phi}_3(t) - \omega_2(t) \quad (32)$$

where $\omega_2(t)$ is a virtual control. The virtual control can be introduced as

$$\omega_2(t) = -h_3\Phi_3(t) \quad (33)$$

where $h_3 > 0$ denotes a constant. Consider a Lyapunov function as follows:

$$W_3(t) = \frac{1}{2}\Phi_3^2(t). \quad (34)$$

Invoking (32)–(34), the time derivative of $W_3(t)$ can be written as

$$\begin{aligned}\dot{W}_3(t) &= \Phi_3(t)\dot{\Phi}_3(t)\\ &= \Phi_3(t)[\Phi_4(t) + \omega_2(t)]\\ &= -h_3\Phi_3^2(t) + \Phi_3(t)\Phi_4(t). \quad (35)\end{aligned}$$

Step 2: Construct the following Lyapunov function:

$$W_4(t) = W_3(t) + \frac{I_m}{2}\Phi_4^2(t). \quad (36)$$

Quoting (14), (32), and (35) yields

$$\begin{aligned}\dot{W}_4(t) =& \dot{W}_3(t) + I_m\Phi_4(t)\dot{\Phi}_4(t)\\ =& -h_3\Phi_3^2(t) + \Phi_3(t)\Phi_4(t) + \Phi_4(t)\\ &\times [\nu_2(t) + \Delta_2 + \tau_d(t) + EIw_{aa}(0,t) - I_m\dot{\omega}_2(t)]. \quad (37)\end{aligned}$$

Therefore, the control law $\nu_2(t)$ can be designed as

$$\begin{aligned}\nu_2(t) =& -h_4\Phi_4(t) - EIw_{aa}(0,t) + I_m\dot{\omega}_2(t) - \Phi_3(t)\\ &- \tau_d(t) - \Delta_2 \quad (38)\end{aligned}$$

with $h_4 > 0$ being a constant.

In the same way, the ANNBC technique is employed to deal with the unknown $\tau_d(t)$ and Δ_2. Invoking Lemma 3, the unknown function Δ_2 can be presented as

$$\Delta_2 = U_2^{*T}\Sigma_2(X_2) + \varepsilon_2^* \quad (39)$$

where U_2^* and ε_2^* are the unknown ideal weight vector and optimal approximation error, respectively, $\Sigma_2(X_2)$ denotes the basis function, and $X_2 = [\Phi_3(t), \Phi_4(t), \dot{\omega}_2(t), w_{aa}(0,t)]$.

According to Lemma 3, it can be drawn that $|\varepsilon_2^*| \leq \bar{\varepsilon}_2^*$, where $\bar{\varepsilon}_2^*$ is an unknown positive constant. Similarly, letting $D_{c2}(t) = \tau_d(t) + \varepsilon_2^*$ and invoking Assumption 1, it has $|D_{c2}(t)| \leq \bar{D}_{c2}$ with $\bar{D}_{c2} > 0$ being an unknown constant. Taking the fact that U_2^* and $\bar{D}_{c2}$ are unknown into consideration, an ANNBC law for the like-posture loop subsystem of the flexible manipulator is given by

$$\dot{\hat{\bar{D}}}_{c2}(t) = -\zeta_3\zeta_4\hat{\bar{D}}_{c2} + \zeta_4\Phi_4(t)\tanh\left(\frac{\Phi_4(t)}{\varsigma_2}\right) \quad (40)$$

$$\dot{\hat{U}}_2(t) = -g_3\left[g_4\hat{U}_2(t) - \Sigma_2(X_2)\Phi_4(t)\right] \quad (41)$$

$$\begin{aligned}\nu_2(t) =& -h_4\Phi_4(t) - EIw_{aa}(0,t) + I_m\dot{\omega}_2(t) - \Phi_3(t)\\ &- \hat{\bar{D}}_{c2}(t)\tanh\left(\frac{\Phi_4(t)}{\varsigma_2}\right) - \hat{U}_2^T(t)\Sigma_2(X_2) \quad (42)\end{aligned}$$

with $\hat{\bar{D}}_{c2}(t)$ and $\hat{U}_2(t)$ denoting the estimations of the unknown $\bar{D}_{c2}$ and U_2^*, respectively, $\zeta_3 > 0$, $\zeta_4 > 0$, $\varsigma_2 > 0$, $g_3 > 0$, and $g_4 > 0$ being constants.

Substituting (39) and (42) into (37), and considering Lemma 2 and $|D_{c2}(t)| \leq \bar{D}_{c2}$, the following is obtained:

$$\begin{aligned}\dot{W}_4(t) \leq& -h_3\Phi_3^2(t) - h_4\Phi_4^2(t) + \tilde{\bar{D}}_{c2}(t)\Phi_4(t)\\ &\times \tanh\left(\frac{\Phi_4(t)}{\varsigma_2}\right) + \Phi_4(t)\tilde{U}_2^T(t)\Sigma_2(X_2)\\ &+ 0.2785\varsigma_2\bar{D}_{c2} \quad (43)\end{aligned}$$

where $\tilde{U}_2(t) = U_2^* - \hat{U}_2(t)$ and $\tilde{\bar{D}}_{c2}(t) = \bar{D}_{c2} - \hat{\bar{D}}_{c2}(t)$.

Next, the Lyapunov function is constructed as

$$W_I(t) = W_4(t) + \frac{1}{2g_3}\tilde{U}_2^T(t)\tilde{U}_2(t) + \frac{1}{2\zeta_4}\tilde{\bar{D}}_{c2}^2(t). \quad (44)$$

Using (40), (41), and (43), and invoking Lemma 1, it can be derived that

$$\begin{aligned}\dot{W}_I(t) =& \dot{W}_4(t) + \frac{1}{g_3}\tilde{U}_2^T(t)\dot{\tilde{U}}_2(t) + \frac{1}{\zeta_4}\tilde{\bar{D}}_{c2}(t)\dot{\tilde{\bar{D}}}_{c2}(t)\\ \leq& -h_3\Phi_3^2(t) - h_4\Phi_4^2(t) - \frac{g_4}{2}\tilde{U}_2^T(t)\tilde{U}_2(t)\\ &- \zeta_3\left(1 - \frac{1}{\pi_4}\right)\tilde{\bar{D}}_{c2}^2(t) + \frac{g_4}{2}U_2^{*T}U_2^* + \zeta_3\pi_4\bar{D}_{c2}^2\\ &+ 0.2785\varsigma_2\bar{D}_{c2} \quad (45)\end{aligned}$$

where $\pi_4 > 0$ is a constant.

C. Convergence Analysis

Based on the proposed controllers represented by (25)–(27) and (40)–(42), the stability of the closed-loop system for the flexible manipulator is summarized as follows.

Theorem 1: Consider the flexible manipulator system depicted by (1), (4), and (11)–(14). Under the ANNBC laws which are described by (25)–(27) and (40)–(42), the closed-loop system of the flexible manipulator is uniformly ultimately bounded. Moreover, the following conclusions hold.

1) The deflection $w(a,t)$ satisfies $\lim_{t\to\infty}|w(a,t)| \le \sqrt{[(2\vartheta_2 r^3)/(\alpha_1 EI\vartheta_1(1-\varphi))]}$.
2) The tracking error $\Phi_3(t)$ of angular displacement $\psi(t)$ converges to a compact set $\Omega = \{\Phi_3(t)||\Phi_3(t)| \le \sqrt{[(2\vartheta_2)/(\vartheta_1(1-\varphi))]}\}$ ultimately,

where

$$\begin{aligned}\vartheta_1 = \min\Bigg\{ & 2h_1 - 2\pi_1 - 2\pi_2 + \alpha_1 EIh_1^2(1-2\pi_6-2\pi_8-2\pi_9)\\ & \frac{2h_2-\alpha_1 EI}{M_p},\ g_1g_2,\ 2\zeta_1\zeta_2\left(1-\frac{1}{\pi_3}\right)\\ & 2h_3 - 4\alpha_1 EI\pi_{10}h_3^2 - 4\mu r^2 h_3^2(\alpha_2\pi_{12}+\alpha_3\pi_{14})\\ & \frac{2\{h_4 - 2\alpha_1 EI\pi_{10} - 2\mu r^2(\alpha_2\pi_{12}+\alpha_3\pi_{14})\}}{I_m}\\ & g_3g_4,\ \frac{\alpha_3\mu - \frac{2\alpha_1}{\pi_5} - \alpha_2\mu - \frac{2\alpha_2\mu r}{\pi_{12}} - \frac{2\alpha_3\mu r}{\pi_{14}}}{\alpha_1\mu(1+\varphi)}\\ & 2\zeta_3\zeta_4\left(1-\frac{1}{\pi_4}\right),\ \frac{2\Xi}{\alpha_1 EI(1+\varphi)}\Bigg\}\\ \vartheta_2 = {} & \frac{g_2}{2}U_1^{*T}U_1^* + \frac{g_4}{2}U_2^{*T}U_2^* + \zeta_1\pi_3\bar{D}_{c1}^2 + 0.2785\varsigma_1\bar{D}_{c1}\\ & + \zeta_3\pi_4\bar{D}_{c2}^2 + 0.2785\varsigma_2\bar{D}_{c2}\\ & + \left\{\alpha_1\pi_5 r + \alpha_2 r^2\pi_{11} + \alpha_3 r^2\pi_{13}\right\}\delta_1^2\\ \varphi = {} & \frac{\max\{\alpha_2\mu r + \alpha_3\mu r, \alpha_2\mu r^3 + \alpha_3\mu r^3\}}{\min\{\alpha_1\mu, \alpha_1 EI\}}\end{aligned}$$

with $\pi_h > 0$, $h = 5,\dots,14$, being constants, $\Xi = (3\alpha_3 EI/2) - (r/\pi_1) - (\alpha_3 r^3/\pi_{13}) - (\alpha_2 r^3/\pi_{11}) - (3\alpha_2 EI/2) - \alpha_1 EIr(\pi_7+\pi_8)$.

Proof: The Lyapunov function candidate is constructed as

$$H(t) = W_O(t) + W_I(t) + H_1(t) + H_2(t) \tag{46}$$

where

$$\begin{aligned}H_1(t) = {} & \frac{\alpha_1\mu}{2}\int_0^r s_t^2(a,t)da\\ & + \frac{\alpha_1 EI}{2}\int_0^r w_{aa}^2(a,t)da \end{aligned}\tag{47}$$

$$\begin{aligned}H_2(t) = {} & \alpha_2\mu\int_0^r (r-a)s_t(a,t)w_a(a,t)da\\ & + \alpha_3\mu\int_0^r as_t(a,t)w_a(a,t)da\end{aligned}\tag{48}$$

where α_1, α_2, and α_3 denote positive constants; moreover, they satisfy $1-\varphi > 0$.

Since the function $H_2(t)$ is made up of two cross-terms, it is not straightforward to show that whether it is positive definite or not. Thus, the process of proof is divided into two steps. First, the following analysis is introduced to illustrate that $H(t)$ can be chosen as a Lyapunov function candidate.

Step 1: Considering (48), it derives that

$$\begin{aligned}|H_2(t)| \le {} & \frac{\alpha_2\mu r}{2}\int_0^r s_t^2(a,t) + w_a^2(a,t)da\\ & + \frac{\alpha_3\mu r}{2}\int_0^r s_t^2(a,t) + w_a^2(a,t)da\\ = {} & \frac{\alpha_2\mu r + \alpha_3\mu r}{2}\int_0^r s_t^2(a,t)da\\ & + \frac{\alpha_2\mu r + \alpha_3\mu r}{2}\int_0^r w_a^2(a,t)da.\end{aligned}\tag{49}$$

According to Lemma 1, it derives that $w_a^2(a,t) \le r\int_0^r w_{aa}^2(a,t)da$. Thus, the inequality (49) can be rewritten as

$$\begin{aligned}|H_2(t)| \le {} & \frac{\alpha_2\mu r + \alpha_3\mu r}{2}\int_0^r s_t^2(a,t)da\\ & + \frac{\alpha_2\mu r^3 + \alpha_3\mu r^3}{2}\int_0^r w_{aa}(a,t)da\\ \le {} & \varphi H_1(t).\end{aligned}\tag{50}$$

Then

$$(1-\varphi)H_1(t) \le H_1(t) + H_2(t) \le (1+\varphi)H_1(t). \tag{51}$$

Since $1-\varphi > 0$, $H(t)$ is positive definite. Hence, $H(t)$ can be chosen as a Lyapunov function.

In the sequel, the convergence of the closed-loop system is analyzed.

Step 2: Combining (1) and (47), and applying Lemma 1, the following is obtained:

$$\begin{aligned}\dot{H}_1(t) = {} & \alpha_1\int_0^r s_t(a,t)\{-EIw_{aaaa}(a,t) + f(a,t)\}da\\ & + \alpha_1 EI\int_0^r w_{aa}(a,t)w_{aat}(a,t)da\\ \le {} & -\alpha_1 EIs_t(r,t)w_{aaa}(r,t) + \alpha_1 EIs_t(0,t)\\ & \times w_{aaa}(0,t) + \alpha_1 EIw_{aa}(r,t)s_{at}(r,t)\\ & - \alpha_1 EIw_{aa}(0,t)s_{at}(0,t)\\ & - \alpha_1 EI\int_0^r w_{aa}(a,t)s_{aat}(a,t)da\\ & + \frac{\alpha_1}{\pi_5}\int_0^r s_t^2(a,t)da + \alpha_1\pi_5\int_0^r f^2(a,t)da\\ & + \alpha_1 EI\int_0^r w_{aa}(a,t)w_{aat}(a,t)da.\end{aligned}\tag{52}$$

Considering the fact that $s(a,t) = a\psi(t) + w(a,t)$, thus $s_{aat}(a,t) = w_{aat}(a,t)$, and invoking $-s_t(r,t)w_{aaa}(r,t) = \frac{1}{2}\Phi_2^2(t) - \frac{1}{2}s_t^2(r,t) - \frac{h_1^2}{2}\Phi_1^2(t) - \frac{1}{2}w_a^2(r,t) - \frac{1}{2}w_{aaa}^2(r,t) - h_1 s_t(r,t)\Phi_1(t) - s_t(r,t)w_a(r,t) + w_a(r,t)w_{aaa}(r,t) - h_1\Phi_1(t)w_a(r,t) + h_1\Phi_1(t)w_{aaa}(r,t)$, $w(0,t) = w_a(0,t) = w_{aa}(r,t) = 0$, (31)–(33) and Lemma 1, it derives

$$\begin{aligned}\dot{H}_1(t) \le {} & \frac{\alpha_1 EI}{2}\Phi_2^2(t) - \frac{\alpha_1 EI}{2}w_a^2(r,t) - \alpha_1 EI\left(\frac{1}{2}-\frac{1}{\pi_9}\right)\\ & \times w_{aaa}^2(r,t) - \alpha_1 EIh_1^2\left(\frac{1}{2}-\pi_6-\pi_8-\pi_9\right)\\ & \times\Phi_1^2(t) - \alpha_1 EI\left(\frac{1}{2}-\frac{1}{\pi_6}-\frac{1}{\pi_7}\right)s_t^2(r,t)\end{aligned}$$

$$+\frac{\alpha_1}{\pi_5}\int_0^r s_t^2(a,t)da+\alpha_1\pi_5\int_0^r f^2(a,t)da$$
$$+\alpha_1 EIr(\pi_7+\pi_8)\int_0^r w_{aa}^2(a,t)da+\frac{\alpha_1 EI}{\pi_{10}}$$
$$\times w_{aa}^2(0,t)+2\alpha_1 EI\pi_{10}\Phi_4^2(t)+2\alpha_1 EI\pi_{10}h_3^2$$
$$\times \Phi_3^2(t)+\alpha_1 EIw_a(r,t)w_{aaa}(r,t). \quad (53)$$

■

Quoting (48), the derivative of $H_2(t)$ is presented by

$$\begin{aligned}\dot H_2(t) &= \alpha_2\mu\int_0^r (r-a)s_{tt}(a,t)w_a(a,t)da\\ &\quad+\alpha_2\mu\int_0^r (r-a)s_t(a,t)w_{at}(a,t)da\\ &\quad+\alpha_3\mu\int_0^r as_{tt}(a,t)w_a(a,t)da\\ &\quad+\alpha_3\mu\int_0^r as_t(a,t)w_{at}(a,t)da\\ &=\dot H_{21}(t)+\dot H_{22}(t)+\dot H_{23}(t)+\dot H_{24}(t)\end{aligned}\quad (54)$$

where

$$\dot H_{21}(t)=\alpha_2\mu\int_0^r (r-a)s_{tt}(a,t)w_a(a,t)da \quad (55)$$
$$\dot H_{22}(t)=\alpha_2\mu\int_0^r (r-a)s_t(a,t)w_{at}(a,t)da \quad (56)$$
$$\dot H_{23}(t)=\alpha_3\mu\int_0^r as_{tt}(a,t)w_a(a,t)da \quad (57)$$
$$\dot H_{24}(t)=\alpha_3\mu\int_0^r as_t(a,t)w_{at}(a,t)da. \quad (58)$$

Utilizing (1) and (55) and using Lemma 1 and $w_a(0,t)=w_{aa}(r,t)=0$, the following is obtained:

$$\begin{aligned}\dot H_{21}(t) &= \alpha_2\int_0^r (r-a)w_a(a,t)\{-EIw_{aaaa}(a,t)+f(a,t)\}da\\ &\le\left(\frac{\alpha_2 r^3}{\pi_{11}}+\frac{3\alpha_2 EI}{2}\right)\int_0^r w_{aa}^2(a,t)da-\frac{\alpha_2 rEI}{2}\\ &\quad\times w_{aa}^2(0,t)+\alpha_2 r\pi_{11}\int_0^r f^2(a,t)da.\end{aligned}\quad (59)$$

According to Lemma 1, $s(a,t)=a\psi(t)+w(a,t)$, $w(0,t)=0$, (31)–(33), and (56), the following is obtained:

$$\begin{aligned}\dot H_{22}(t) &= \alpha_2\mu\int_0^r (r-a)s_t(a,t)\big[s_{at}(a,t)-\dot\psi(t)\big]da\\ &\le\alpha_2\mu\left(\frac{1}{2}+\frac{r}{\pi_{12}}\right)\int_0^r s_t^2(a,t)da+2\alpha_2\mu r^2\pi_{12}\\ &\quad\times\Phi_4^2+2\alpha_2\mu r^2\pi_{12}h_3^2\Phi_3^2.\end{aligned}\quad (60)$$

Applying (1), (57), and Lemma 1 and invoking $w_a(0,t)=w_{aa}(r,t)=0$, the following is obtained:

$$\begin{aligned}\dot H_{23}(t) &= \alpha_3\int_0^r aw_a(a,t)\{-EIw_{aaaa}(a,t)+f(a,t)\}da\\ &\le -\alpha_3 EIrw_a(r,t)w_{aaa}(r,t)-\alpha_3\left(\frac{3EI}{2}-\frac{r^3}{\pi_{13}}\right)\\ &\quad\times\int_0^r w_{aa}^2(a,t)da+\alpha_3 r\pi_{13}\int_0^r f^2(a,t)da.\end{aligned}\quad (61)$$

Invoking (31)–(33), (58), $s(a,t)=a\psi(t)+w(a,t)$, and Lemma 1, the following holds:

$$\begin{aligned}\dot H_{24}(t) &= \alpha_3\mu\int_0^r as_t(a,t)\big[s_{at}(a,t)-\dot\psi(t)\big]da\\ &\le\frac{\alpha_3\mu r}{2}s_t^2(r,t)-\alpha_3\mu\left(\frac{1}{2}-\frac{r}{\pi_{14}}\right)\int_0^r s_t^2(a,t)da\\ &\quad+2\alpha_3\mu r^2\pi_{14}h_3^2\Phi_3^2(t)+2\alpha_3\mu r^2\pi_{14}\Phi_4^2(t).\end{aligned}\quad (62)$$

Substituting (59)–(62) into (54), the following is obtained:

$$\begin{aligned}\dot H_2(t) &\le -\left(\frac{3\alpha_3 EI}{2}-\frac{\alpha_3 r^3}{\pi_{13}}-\frac{\alpha_2 r^3}{\pi_{11}}-\frac{3\alpha_2 EI}{2}\right)\\ &\quad\times\int_0^r w_{aa}^2(a,t)da\\ &\quad-\left(\frac{\alpha_3\mu}{2}-\frac{\alpha_3\mu r}{\pi_{14}}-\frac{\alpha_2\mu}{2}-\frac{\alpha_2\mu r}{\pi_{12}}\right)\\ &\quad\times\int_0^r s_t^2(a,t)da+2\mu r^2h_3^2(\alpha_2\pi_{12}+\alpha_3\pi_{14})\Phi_3^2\\ &\quad+2\mu r^2(\alpha_2\pi_{12}+\alpha_3\pi_{14})\Phi_4^2\\ &\quad-\frac{\alpha_2 rEI}{2}w_{aa}^2(0,t)-\alpha_3 EIrw_a(r,t)w_{aaa}(r,t)\\ &\quad+(\alpha_2 r\pi_{11}+\alpha_3 r\pi_{13})\int_0^r f^2(a,t)da\\ &\quad+\frac{\alpha_3\mu r}{2}s_t^2(r,t).\end{aligned}\quad (63)$$

Quoting (30), (45), (46), (53), and (63) and considering Assumption 1 and $\alpha_1 EIw_a(r,t)w_{aaa}(r,t)-\alpha_3 EIrw_a(r,t)\times w_{aaa}(r,t)\le[(|\alpha_1 EI-\alpha_3 EIr|)/\pi_{15}]w_a^2(r,t)+\pi_{15}|\alpha_1 EI-\alpha_3 EIr|w_{aaa}^2(r,t)$, the following inequality is derived:

$$\begin{aligned}\dot H(t) &\le -\left\{h_1-\pi_1+\alpha_1 EIh_1^2\left(\frac{1}{2}-\pi_6-\pi_8-\pi_9\right)-\pi_2\right\}\\ &\quad\times\Phi_1^2(t)-\left\{h_2-\frac{\alpha_1 EI}{2}\right\}\Phi_2^2(t)-\frac{g_2}{2}\tilde U_1^T(t)\\ &\quad\times\tilde U_1(t)-\zeta_1\left(1-\frac{1}{\pi_3}\right)\tilde{\tilde D}_{c1}^2(t)\\ &\quad-\left\{h_3-2\alpha_1 EI\pi_{10}h_3^2-2\mu r^2h_3^2(\alpha_2\pi_{12}+\alpha_3\pi_{14})\right\}\\ &\quad\times\Phi_3^2-\left\{h_4-2\alpha_1 EI\pi_{10}-2\mu r^2(\alpha_2\pi_{12}+\alpha_3\pi_{14})\right\}\\ &\quad\times\Phi_4^2(t)-\frac{g_4}{2}\tilde U_2^T(t)\tilde U_2(t)-\zeta_3\left(1-\frac{1}{\pi_4}\right)\tilde{\tilde D}_{c2}^2(t)\\ &\quad-\left\{\frac{\alpha_3\mu}{2}-\frac{\alpha_2\mu}{2}-\frac{\alpha_1}{\pi_5}-\frac{\alpha_2\mu r}{\pi_{12}}-\frac{\alpha_3\mu r}{\pi_{14}}\right\}\\ &\quad\times\int_0^r s_t^2(a,t)da\\ &\quad-\left\{\frac{3\alpha_3 EI}{2}-\frac{3\alpha_2 EI}{2}-\frac{r}{\pi_1}-\alpha_1 EIr(\pi_7+\pi_8)\right.\\ &\qquad\left.-\frac{\alpha_2 r^3}{\pi_{11}}-\frac{\alpha_3 r^3}{\pi_{13}}\right\}\int_0^r w_{aa}^2(a,t)da\\ &\quad-\left\{\alpha_1 EI\left(\frac{1}{2}-\frac{1}{\pi_6}-\frac{1}{\pi_7}\right)-\frac{\alpha_3\mu r}{2}\right\}s_t^2(r,t)\\ &\quad-\left\{\alpha_1 EI\left(\frac{1}{2}-\frac{1}{\pi_9}\right)-\pi_{15}|\alpha_1 EI-\alpha_3 EIr|-\frac{1}{\pi_2}\right\}\\ &\quad\times w_{aaa}^2(r,t)-\left\{\frac{\alpha_1 EI}{2}-\frac{|\alpha_1 EI-\alpha_3 EIr|}{\pi_{15}}\right\}\end{aligned}$$

$$\begin{aligned}&\times\ w_a^2(r,t)-\left\{\frac{\alpha_2 rEI}{2}-\frac{\alpha_1 EI}{\pi_{10}}\right\}w_{aa}^2(0,t)+\frac{g_2}{2}\\&\times\ U_1^{*T}U_1^*+\frac{g_4}{2}U_2^{*T}U_2^*+\zeta_1\pi_3\bar{D}_{c1}^2+0.2785\varsigma_1\bar{D}_{c1}\\&+\ \zeta_3\pi_4\bar{D}_{c2}^2+0.2785\varsigma_2\bar{D}_{c2}\\&+\ \left\{\alpha_1\pi_5 r+\alpha_2 r^2\pi_{11}+\alpha_3 r^2\pi_{13}\right\}\delta_1^2\\&\leq -\vartheta_1 H(t)+\vartheta_2\end{aligned}\tag{64}$$

where the following conditions hold:

$$h_1-\pi_1-\pi_2+\alpha_1 EIh_1^2\left(\frac{1}{2}-\pi_6-\pi_8-\pi_9\right)>0\tag{65}$$

$$h_2-\frac{\alpha_1 EI}{2}>0,\ 1-\frac{1}{\pi_3}>0,\ 1-\frac{1}{\pi_4}>0\tag{66}$$

$$h_3-2\alpha_1 EI\pi_{10}h_3^2-2\mu r^2h_3^2(\alpha_2\pi_{12}+\alpha_3\pi_{14})>0\tag{67}$$

$$h_4-2\alpha_1 EI\pi_{10}-2\mu r^2(\alpha_2\pi_{12}+\alpha_3\pi_{14})>0\tag{68}$$

$$\frac{\alpha_3\mu}{2}-\frac{\alpha_1}{\pi_5}-\frac{\alpha_2\mu}{2}-\frac{\alpha_2\mu r}{\pi_{12}}-\frac{\alpha_3\mu r}{\pi_{14}}>0,\ \Xi>0\tag{69}$$

$$\alpha_1 EI\left(\frac{1}{2}-\frac{1}{\pi_6}-\frac{1}{\pi_7}\right)-\frac{\alpha_3\mu r}{2}\geq 0\tag{70}$$

$$\alpha_1 EI\left(\frac{1}{2}-\frac{1}{\pi_9}\right)-\frac{1}{\pi_2}-\pi_{15}|\alpha_1 EI-\alpha_3 EIr|\geq 0\tag{71}$$

$$\frac{\alpha_1 EI}{2}-\frac{|\alpha_1 EI-\alpha_3 EIr|}{\pi_{15}}\geq 0,\ \frac{\alpha_2 rEI}{2}-\frac{\alpha_1 EI}{\pi_{10}}\geq 0\tag{72}$$

with $\pi_{15}>0$ being a constant.

From (64), the following holds:

$$\frac{d\left(H(t)e^{\vartheta_1 t}\right)}{dt}\leq\vartheta_2 e^{\vartheta_1 t}\tag{73}$$

furthermore

$$H(t)\leq H(0)e^{-\vartheta_1 t}+\frac{\vartheta_2}{\vartheta_1}.\tag{74}$$

According to Lemma 1, it derives that

$$\frac{\alpha_1 EI}{2}w^2(a,t)\leq r^3\frac{\alpha_1 EI}{2}\int_0^r w_{aa}^2(a,t)da.\tag{75}$$

Invoking (46)–(48), (51), (74), and (75), it has

$$\frac{\alpha_1 EI}{2}w^2(a,t)\leq\frac{H(0)e^{-\vartheta_1 t}r^3}{1-\varphi}+\frac{\vartheta_2 r^3}{\vartheta_1(1-\varphi)}.\tag{76}$$

Thus, when $t\to\infty$

$$|w(a,t)|\leq\sqrt{\frac{2\vartheta_2 r^3}{\alpha_1 EI\vartheta_1(1-\varphi)}}.\tag{77}$$

Quoting (34), (36), (44), (46), (51), and (74) yields

$$\begin{aligned}\frac{1}{2}\Phi_3^2(t)&\leq\frac{H(t)}{1-\varphi}\\&\leq\frac{H(0)e^{-\vartheta_1 t}+\frac{\vartheta_2}{\vartheta_1}}{1-\varphi}\end{aligned}\tag{78}$$

then, when $t\to\infty$

$$|\Phi_3(t)|\leq\sqrt{\frac{2\vartheta_2}{\vartheta_1(1-\varphi)}}.\tag{79}$$

That is, the tracking error $\Phi_3(t)$ of angular displacement $\psi(t)$ converges to a compact set $\Omega=\{\Phi_3(t)||\Phi_3(t)|\leq\sqrt{[2\vartheta_2/(\vartheta_1(1-\varphi))]}\}$ ultimately.

Remark 4: The design parameters h_{q_1}, $q_1=1,2,3,4$, in (27) and (42) should take the system model parameters, $1-[(\max\{\alpha_2\mu r+\alpha_3\mu r,\alpha_2\mu r^3+\alpha_3\mu r^3\})/(\min\{\alpha_1\mu,\alpha_1 EI\})]>0$ and the inequalities (65)–(72) into consideration, that is, the designs for h_{q_1} are motivated by the completeness of the stability conditions. Moreover, the parameters ζ_{q_2}, g_{q_3}, ς_1, and ς_2 in (25), (26), (40), and (41) need to be designed based on experiences, $q_2,q_3=1,2,3,4$.

IV. Numerical Simulation

In this section, we consider the flexible manipulator system given by (1), (4), and (11)–(14). A numerical simulation is performed to check the control performance of the derived ANNBC laws (25)–(27) and (40)–(42). The parameters of the flexible manipulator are given by: $r=1.0$ m, $EI=2.0$ N $\cdot$m^2, $\mu=0.2$ kg/m, $M_p=0.25$ kg, and $I_m=0.4$ kg$\cdot$m^2. The external disturbances are described as follows: $f(a,t)=(1.2+0.4\sin(0.1\pi t)+0.2\sin(0.2\pi t)+0.1\sin(0.4\pi t))a/10$, $d(t)=1.0+0.2\sin(0.1t)+0.3\sin(0.3t)+0.4\sin(0.5t)$, and $\tau_d(t)=1.0+0.2\sin(0.1t)+0.3\sin(0.3t)+0.4\sin(0.5t)$.

The saturation levels $\kappa_{M1}=2.1$, $\kappa_{M2}=2.1$, $\kappa_{m1}=-2.1$, and $\kappa_{m2}=-1.95$, the dead-zone ranges $m_{li}=-0.1$ and $m_{ri}=0.1$, and the slope parameters $k_{li}=1.0$ and $k_{ri}=1.0$, $i=1,2$. The model uncertainties are considered as follows: $\Delta f_1=-0.2EIw_{aaa}(r,t)$ and $\Delta f_2=-0.2EIw_{aa}(0,t)$. The reference signal of the angular displacement is $\psi_r(t)=0.6$ rad.

The initial values of the flexible manipulator are described by $w(a,0)=0$, $\dot{w}(a,0)=0$, and $\psi(0)=0$. The simulation results are listed by two scenarios.

Scenario I: With the proposed ANNBC.

The radial basis functions of RBFNN are chosen as Gaussian functions described as [39]

$$\Sigma_1(X_1)=[\Sigma_{11},\Sigma_{12},\ldots,\Sigma_{19}]^T\tag{80}$$

$$\Sigma_2(X_2)=[\Sigma_{21},\Sigma_{22},\ldots,\Sigma_{29}]^T\tag{81}$$

where $\Sigma_{1j}=\exp([(-(X_1-c_j)^T(X_1-c_j))/(b_j^2)])$ and $\Sigma_{2k}=\exp([(-(X_2-x_k)^T(X_2-x_k))/y_k^2])$ with c_j and x_k denoting the center of the neural cell of the jth hidden layer and kth hidden layer, respectively, and b_j and y_k being the width of the neural cell of the jth hidden layer and kth hidden layer, respectively, $j,k=1,2,\ldots,9$.

The design parameters of the ANNBC scenario are given by $\zeta_1=0.001$, $\zeta_2=1.0$, $\zeta_3=0.001$, $\zeta_4=1.0$, $g_1=2.0$, $g_2=0.2$, $g_3=1.0$, $g_2=0.5$, $\varsigma_1=0.01$, $\varsigma_2=0.01$, $h_1=0.1$, $h_2=15$, $h_3=3.0$, and $h_4=5.0$.

Under the ANNBC scheme depicted by (25)–(27) and (40)–(42), the response curves of the closed-loop system for the flexible manipulator are shown by Figs. 2–5. Fig. 2 shows the deflection $w(a,t)$ of the flexible manipulator. Specifically, when $a=r/2$ and $a=r$, the simulation curve is given by Fig. 3. Fig. 4 exhibits the angular displacement tracking error $\Phi_3(t)$ of the flexible manipulator, which is followed by the designed ANNBC inputs and actuator outputs in

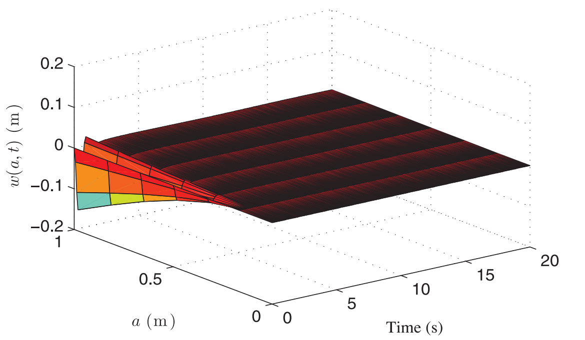

Fig. 2. Deflection $w(a, t)$ of the flexible manipulator with the ANNBC.

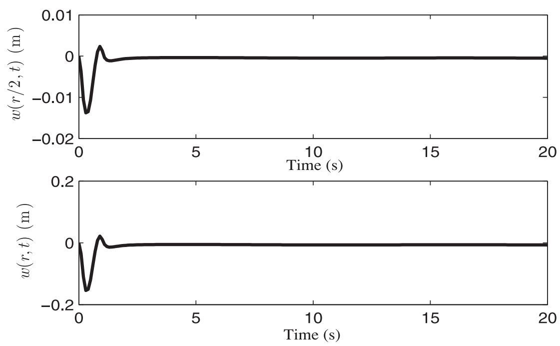

Fig. 3. Deflection of the flexible manipulator at $a = r/2$ and $a = r$ with the ANNBC.

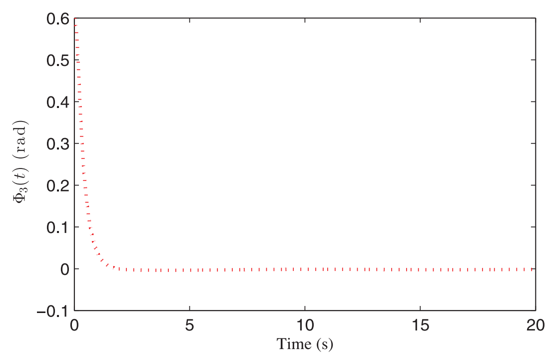

Fig. 4. Angular displacement tracking error $\Phi_3(t)$ with the ANNBC.

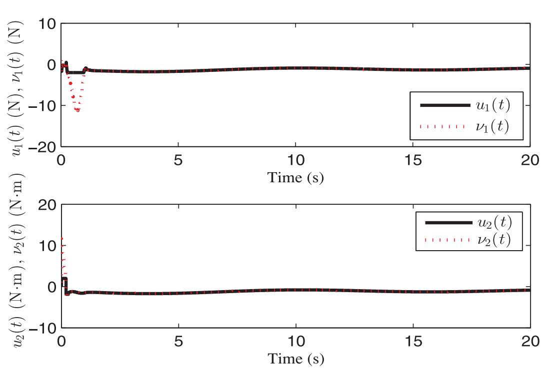

Fig. 5. Control laws with the ANNBC.

Fig. 5. The solid line and dotted line denote the actuator outputs $u_i(t)$ and the designed ANNBC inputs $\nu_i(t)$, respectively, $i = 1, 2$.

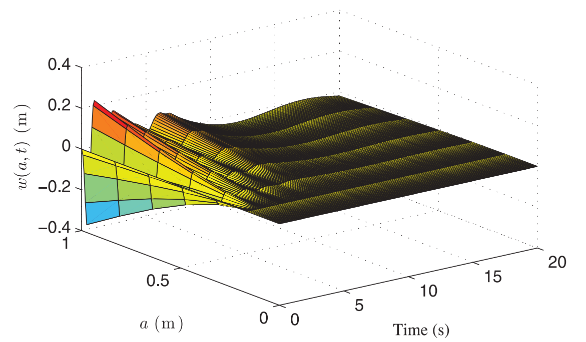

Fig. 6. Deflection $w(a, t)$ of the flexible manipulator with a PD control.

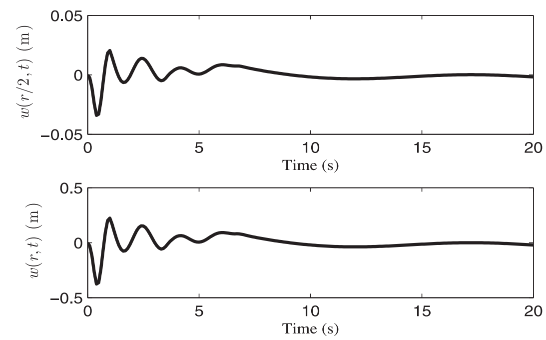

Fig. 7. Deflection of the flexible manipulator at $a = r/2$ and $a = r$ with a PD control.

From Figs. 2–5, it is obvious that the deflection $w(a, t)$ and angular displacement tracking error $\Phi_3(t)$ can converge to a small neighborhood of origin quickly. Thus, the performance robustness of the closed-loop system for the flexible manipulator against input constraints, model uncertainties, and external disturbances is strong with the developed ANNBC.

Scenario II: With a PD control.

The PD control is introduced as follows:

$$u_1(t) = -l_1 z_1(t) - l_2 z_2(t) \tag{82}$$

$$u_2(t) = -l_3 z_3(t) - l_4 z_4(t) \tag{83}$$

with $l_1 > 0$, $l_2 > 0$, $l_3 > 0$, and $l_4 > 0$ representing constants. The design parameters are listed as follows: $l_1 = 2.0$, $l_2 = 10$, $l_3 = 30$, and $l_4 = 5.0$.

Under the PD control, the simulation response curves of the flexible manipulator are given by Figs. 6–9. Fig. 6 is the dynamic figure of the deflection $w(a, t)$. Concretely, Fig. 7 shows the deflection curves at $a = r/2$ and $a = r$ of the flexible manipulator. The angular displacement tracking error $\Phi_3(t)$ is represented by Fig. 8. Fig. 9 presents the actuator outputs $u_i(t)$ and the designed control laws $\nu_i(t)$ by adopting the PD control, $i = 1, 2$.

Comparing Figs. 2–4 with Figs. 6–8, respectively, it can be seen that the control performance by employing the introduced ANNBC is better than that of the PD control. It mainly reflects in the following two aspects.

1) In comparison to a PD control, the deflection $w(a, t)$ and angular displacement tracking error $\Phi_3(t)$ can converge to a smaller neighborhood of the origin by using the ANNBC.

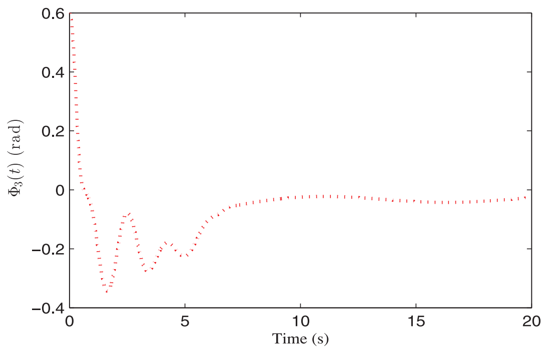

Fig. 8. Angular displacement tracking error $\Phi_3(t)$ with a PD control.

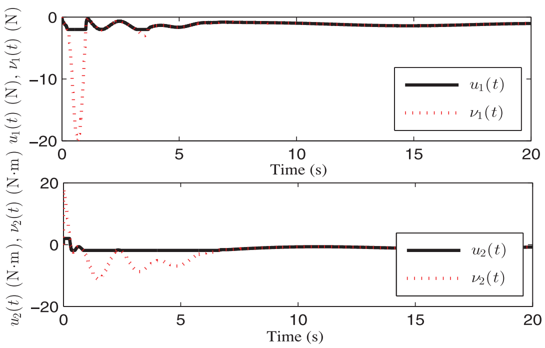

Fig. 9. Control laws with a PD control.

2) In contrast to a PD control, it takes less time to be convergent to a small neighborhood of the origin with the ANNBC.

In short, the validity of the proposed ANNBC is proved in accordance with the aforementioned simulation results. Meanwhile, comparing with a PD control, better control performance can be achieved by using the ANNBC for the considered flexible manipulator system.

V. Conclusion

The ANNBC laws have been derived for the flexible manipulator with input nonlinearities, model uncertainties, and external disturbances in this article. The problem of input saturation and input dead zone has been transformed into a new problem of input saturation. For unknown model uncertainties and new saturation errors, the technology of RBFNN has been utilized to approximate them. With the outputs of RBFNN and the strategy of the backstepping, the ANNBC laws have been designed to restrain vibration and to track the desired angular displacement of the flexible manipulator. The validity of the developed ANNBC has been verified by numerical simulation. In the future, the deflection suppression and angular displacement tracking control will be addressed for a 3-D flexible manipulator and an axially moving flexible manipulator [58], [59].

References

[1] S. Chen, Z. Zhao, D. Zhu, C. Zhang, and H. Li, "Adaptive robust control for a spatial flexible Timoshenko manipulator subject to input dead-zone," *IEEE Trans. Syst., Man, Cybern., Syst.*, early access, 2020, doi: 10.1109/TSMC.2020.3020326.

[2] Z. Zhao and Z. Li, "Finite-time convergence disturbance rejection control for a flexible Timoshenko manipulator," *IEEE/CAA J. Automatica Sinica*, early access, 2020, doi: 10.1109/JAS.2020.1003378.

[3] L. Tian and C. Collins, "Adaptive neuro-fuzzy control of a flexible manipulator," *Mechatronics*, vol. 15, no. 10, pp. 1305–1320, 2005.

[4] J. Wei, Z. Qiu, and Y. Wang, "Experimental comparison research on active vibration control for flexible piezoelectric manipulator using fuzzy controller," *J. Intell. Robot. Syst.*, vol. 59, no. 1, pp. 31–56, 2010.

[5] W. He, Y. Ouyang, and J. Hong, "Vibration control of a flexible robotic manipulator in the presence of input deadzone," *IEEE Trans. Ind. Informat.*, vol. 13, no. 1, pp. 48–59, Feb. 2017.

[6] C. Sun, W. He, and J. Hong, "Neural network control of a flexible robotic manipulator using the lumped spring-mass model," *IEEE Trans. Syst., Man, Cybern., Syst.*, vol. 47, no. 8, pp. 1863–1874, Aug. 2017.

[7] W. He, H. Gao, C. Zhou, C. Yang, and Z. Li, "Reinforcement learning control of a flexible two-link manipulator: An experimental investigation," *IEEE Trans. Syst., Man, Cybern., Syst.*, early access, Mar. 5, 2020, doi: 10.1109/TSMC.2020.2975232.

[8] Z. Zhao and C. Ahn, "Boundary output constrained control for a flexible beam system with prescribed performance," *IEEE Trans. Syst., Man, Cybern., Syst.*, early access, Oct. 18, 2019, doi: 10.1109/TSMC.2019.2944900.

[9] X. He, Z. Zhao, J. Su, Q. Yang, and D. Zhu, "Adaptive inverse control of a vibrating coupled vessel-riser system with input backlash," *IEEE Trans. Syst., Man, Cybern., Syst.*, early access, Oct. 17, 2019, doi: 10.1109/TSMC.2019.2944999.

[10] W. He, T. Meng, X. He, and C. Sun, "Iterative learning control for a flapping wing micro aerial vehicle under distributed disturbances," *IEEE Trans. Cybern.*, vol. 49, no. 4, pp. 1524–1535, Apr. 2019.

[11] W. He, T. Wang, X. He, L.-J. Yang, and O. Kaynak, "Dynamical modeling and boundary vibration control of a rigid-flexible wing system," *IEEE/ASME Trans. Mechatronics*, early access, Apr. 21, 2020, doi: 10.1109/TMECH.2020.2987963.

[12] Z. Liu, J. Liu, and W. He, "Modeling and vibration control of a flexible aerial refueling hose with variable lengths and input constraint," *Automatica*, vol. 77, pp. 302–310, Mar. 2017.

[13] Z. Zhao, S. Lin, D. Zhu, and G. Wen, "Vibration control of a riser-vessel system subject to input backlash and extraneous disturbances," *IEEE Trans. Circuits Syst. II, Exp. Briefs*, vol. 67, no. 3, pp. 516–520, Mar. 2020.

[14] Z. Liu, Z. Zhao, and C. K. Ahn, "Boundary constrained control of flexible string systems subject to disturbances," *IEEE Trans. Circuits Syst. II, Exp. Briefs*, vol. 67, no. 1, pp. 112–116, Jan. 2020.

[15] Z. Zhao, C. K. Ahn, and H. X. Li, "Boundary antidisturbance control of a spatially nonlinear flexible string system," *IEEE Trans. Ind. Electron.*, vol. 67, no. 6, pp. 4846–4856, Jun. 2020.

[16] Y. Ren and M. Chen, "Anti-swing control for a suspension cable system of a helicopter with cable swing constraint and unknown dead-zone," *Neurocomputing*, vol. 356, pp. 257–267, Sep. 2019.

[17] Y. Ren, M. Chen, and J. Liu, "Unilateral boundary control for a suspension cable system of a helicopter with horizontal motion," *IET Control Theory Appl.*, vol. 13, no. 4, pp. 467–476, Mar. 2019.

[18] M. Chen, Y. Ren, and J. Liu, "Antidisturbance control for a suspension cable system of helicopter subject to input nonlinearities," *IEEE Trans. Syst., Man, Cybern., Syst.*, vol. 48, no. 12, pp. 2292–2304, Dec. 2018.

[19] Z. Zhao, X. He, Z. Ren, and G. Wen, "Boundary adaptive robust control of a flexible riser system with input nonlinearities," *IEEE Trans. Syst., Man, Cybern., Syst.*, vol. 49, no. 10, pp. 1971–1980, Oct. 2019.

[20] Z. Zhao, C. K. Ahn, and H.-X. Li, "Dead zone compensation and adaptive vibration control of uncertain spatial flexible riser systems," *IEEE/ASME Trans. Mechatronics*, vol. 25, no. 3, pp. 1398–1408, Jun. 2020.

[21] Z. Zhao, X. He, Z. Ren, and G. Wen, "Output feedback stabilization for an axially moving system," *IEEE Trans. Syst., Man, Cybern., Syst.*, vol. 49, no. 12, pp. 2374–2383, Dec. 2019.

[22] X. He, W. He, J. Shi, and C. Sun, "Boundary vibration control of variable length crane systems in two-dimensional space with output constraints," *IEEE/ASME Trans. Mechatronics*, vol. 22, no. 5, pp. 1952–1962, Oct. 2017.

[23] Y. Liu, Y. Fu, W. He, and Q. Hui, "Modeling and observer-based vibration control of a flexible spacecraft with external disturbances," *IEEE Trans. Ind. Electron.*, vol. 66, no. 11, pp. 8648–8658, Nov. 2019.

[24] Z. Liu, X. He, Z. Zhao, C. K. Ahn, and H.-X. Li, "Vibration control for spatial aerial refueling hoses with bounded actuators," *IEEE Trans. Ind. Electron.*, early access, Apr. 9, 2020, doi: 10.1109/TIE.2020.2984442.

[25] T. Zhang, C. L. P. Chen, L. Chen, X. Xu, and B. Hu, "Design of highly nonlinear substitution boxes based on I-ching operators," *IEEE Trans. Cybern.*, vol. 48, no. 12, pp. 3349–3358, Dec. 2018.
[26] T. Zhang, X. Wang, X. Xu, and C. L. P. Chen, "GCB-Net: Graph convolutional broad network and its application in emotion recognition," *IEEE Trans. Affective Comput.*, early access, Aug. 27, 2019, doi: 10.1109/TAFFC.2019.2937768.
[27] L. Liu, Y.-J. Liu, and S. Tong, "Neural networks-based adaptive finite-time fault-tolerant control for a class of strict-feedback switched nonlinear systems," *IEEE Trans. Cybern.*, vol. 49, no. 7, pp. 2536–2545, Jul. 2019.
[28] D.-P. Li, Y.-J. Liu, S. Tong, C. L. P. Chen, and D.-J. Li, "Neural networks-based adaptive control for nonlinear state constrained systems with input delay," *IEEE Trans. Cybern.*, vol. 49, no. 4, pp. 1249–1258, Apr. 2019.
[29] Q. Wei, D. Wang, and D. Zhang, "Dual iterative adaptive dynamic programming for a class of discrete-time nonlinear systems with time-delays," *Neural Comput. Appl.*, vol. 23, nos. 7–8, pp. 1851–1863, 2013.
[30] Q. Yang, Z. Yang, and Y. Sun, "Universal neural network control of MIMO uncertain nonlinear systems," *IEEE Trans. Neural Netw. Learn. Syst.*, vol. 23, no. 7, pp. 1163–1169, Jul. 2012.
[31] Q. Yang, S. S. Ge, and Y. Sun, "Adaptive actuator fault tolerant control for uncertain nonlinear systems with multiple actuators," *Automatica*, vol. 60, pp. 92–99, Oct. 2015.
[32] X. Zhong, H. He, D. Wang, and Z. Ni, "Model-free adaptive control for unknown nonlinear zero-sum differential game," *IEEE Trans. Cybern.*, vol. 48, no. 5, pp. 1633–1646, May 2018.
[33] Y. Yang, W. He, Q.-L. Han, and C. Peng, "H_∞ synchronization of networked master–slave oscillators with delayed position data: The positive effects of network-induced delays," *IEEE Trans. Cybern.*, vol. 49, no. 12, pp. 4090–4102, Dec. 2019.
[34] C. Yang, G. Peng, Y. Li, R. Cui, L. Cheng, and Z. Li, "Neural networks enhanced adaptive admittance control of optimized robot–environment interaction," *IEEE Trans. Cybern.*, vol. 49, no. 7, pp. 2568–2579, Jul. 2019.
[35] C. Yang, G. Peng, L. Cheng, J. Na, and Z. Li, "Force sensorless admittance control for teleoperation of uncertain robot manipulator using neural networks," *IEEE Trans. Syst., Man, Cybern., Syst.*, early access, Jun. 28, 2019, doi: 10.1109/TSMC.2019.2920870.
[36] S. He, M. Wang, S.-L. Dai, and F. Luo, "Leader–follower formation control of USVs with prescribed performance and collision avoidance," *IEEE Trans. Ind. Informat.*, vol. 15, no. 1, pp. 572–581, Jan. 2019.
[37] M. Wang, Z. Wang, Y. Chen, and W. Sheng, "Adaptive neural event-triggered control for discrete-time strict-feedback nonlinear systems," *IEEE Trans. Cybern.*, vol. 50, no. 7, pp. 2946–2958, Jul. 2020.
[38] M. Chen, S. S. Ge, and B. V. E. How, "Robust adaptive neural network control for a class of uncertain MIMO nonlinear systems with input nonlinearities," *IEEE Trans. Neural Netw.*, vol. 21, no. 5, pp. 796–812, May 2010.
[39] M. Chen, G. Tao, and B. Jiang, "Dynamic surface control using neural networks for a class of uncertain nonlinear systems with input saturation," *IEEE Trans. Neural Netw. Learn. Syst.*, vol. 26, no. 9, pp. 2086–2097, Sep. 2015.
[40] C. Yang, X. Wang, Z. Li, Y. Li, and C.-Y. Su, "Teleoperation control based on combination of wave variable and neural networks," *IEEE Trans. Syst., Man, Cybern., Syst.*, vol. 47, no. 8, pp. 2125–2136, Aug. 2017.
[41] P. Du, H. Liang, S. Zhao, and C. K. Ahn, "Neural-based decentralized adaptive finite-time control for nonlinear large-scale systems with time-varying output constraints," *IEEE Trans. Syst., Man, Cybern., Syst.*, early access, Jun. 13, 2019, doi: 10.1109/TSMC.2019.2918351.
[42] B. Niu, Y. Liu, W. Zhou, H. Li, P. Duan, and J. Li, "Multiple Lyapunov functions for adaptive neural tracking control of switched nonlinear nonlower-triangular systems," *IEEE Trans. Cybern.*, vol. 50, no. 5, pp. 1877–1886, May 2020.
[43] H. Y. Li, S. Y. Zhao, W. He, and R. Q. Lu, "Adaptive finite-time tracking control of full states constrained nonlinear systems with dead-zone," *Automatica*, vol. 100, pp. 99–107, Feb. 2019.
[44] S. Zhang, Y. Dong, Y. Ouyang, Z. Yin, and K. Peng, "Adaptive neural control for robotic manipulators with output constraints and uncertainties," *IEEE Trans. Neural Netw. Learn. Syst.*, vol. 29, no. 11, pp. 5554–5564, Nov. 2018.
[45] L. Kong, W. He, Y. Dong, L. Cheng, C. Yang, and Z. Li, "Asymmetric bounded neural control for an uncertain robot by state feedback and output feedback," *IEEE Trans. Syst., Man, Cybern., Syst.*, early access, Apr. 4, 2019, doi: 10.1109/TSMC.2019.2901277.
[46] W. He, Y. Sun, Z. Yan, C. Yang, Z. Li, and O. Kaynak, "Disturbance observer-based neural network control of cooperative multiple manipulators with input saturation," *IEEE Trans. Neural Netw. Learn. Syst.*, vol. 31, no. 5, pp. 1735–1746, May 2020.
[47] H. Gao, W. He, Y. Song, S. Zhang, and C. Sun, "Modeling and neural network control of a flexible beam with unknown spatiotemporally varying disturbance using assumed mode method," *Neurocomputing*, vol. 314, pp. 458–467, Nov. 2018.
[48] Q. Hu and B. Xiao, "Intelligent proportional-derivative control for flexible spacecraft attitude stabilization with unknown input saturation," *Aerosp. Sci. Technol.*, vol. 23, no. 1, pp. 63–74, 2012.
[49] Z. Zhao, X. Wang, C. Zhang, Z. Liu, and J. Yang, "Neural network based boundary control of a vibrating string system with input deadzone," *Neurocomputing*, vol. 275, pp. 1021–1027, Jan. 2018.
[50] W. He, X. He, M. Zou, and H. Li, "PDE model-based boundary control design for a flexible robotic manipulator with input backlash," *IEEE Trans. Control Syst. Technol.*, vol. 27, no. 2, pp. 790–797, Mar. 2019.
[51] X. He, Z. Zhao, and Y. Song, "Active control for flexible mechanical systems with mixed deadzone-saturation input nonlinearities and output constraint," *J. Franklin Inst.*, vol. 356, no. 9, pp. 4749–4772, 2019.
[52] Z. Zhao, X. He, and C. K. Ahn, "Boundary disturbance observer-based control of a vibrating single-link flexible manipulator," *IEEE Trans. Syst., Man, Cybern., Syst.*, early access, May 7, 2019, doi: 10.1109/TSMC.2019.2912900.
[53] Z. Liu, J. Liu, and W. He, "Adaptive boundary control of a flexible manipulator with input saturation," *Int. J. Control*, vol. 89, no. 6, pp. 1191–1202, 2016.
[54] M. C. R. Liñán and W. P. Heath, "Controller structure for plants with combined saturation and deadzone/backlash," in *Proc. IEEE Int. Conf. Control Appl.*, Dubrovnik, Croatia, 2012, pp. 1394–1399.
[55] G. H. Hardy, J. E. Littlewood, and G. Polya, *Inequalities*. Cambridge, U.K.: Cambridge Univ. Press, 1959.
[56] M. Chen, P. Shi, and C. C. Lim, "Adaptive neural fault-tolerant control of a 3-DOF model helicopter system," *IEEE Trans. Syst., Man, Cybern., Syst.*, vol. 46, no. 2, pp. 260–270, Feb. 2016.
[57] S. S. Ge, T. H. Lee, G. Zhu, and F. Hong, "Variable structure control of a distributed-parameter flexible beam," *J. Robot. Syst.*, vol. 18, no. 1, pp. 17–27, 2001.
[58] K.-S. Hong and P.-T. Pham, "Control of axially moving systems: A review," *Int. J. Control Autom. Syst.*, vol. 17, no. 12, pp. 2983–3008, 2019.
[59] P.-T. Pham and K.-S. Hong, "Dynamic models of axially moving systems: A review," *Nonlinear Dyn.*, vol. 100, no. 1, pp. 315–349, 2020.

Yong Ren received the M.Sc. degree from the Institute of Automation, Qufu Normal University, Qufu, China, in 2015, and the Ph.D. degree from the College of Automation Engineering, Nanjing University of Aeronautics and Astronautics, Nanjing, China, in 2019.

He is currently a Lecturer with the College of Electrical Engineering and Automation, Shandong University of Science and Technology, Qingdao, China. His current research interests include adaptive control, fault-tolerant control, DPSs, and robotic systems.

Zhijia Zhao (Member, IEEE) received the B.Eng. degree in automatic control from the North China University of Water Resources and Electric Power, Zhengzhou, China, in 2010, and the M.Eng. and Ph.D. degrees in automatic control from the South China University of Technology, Guangzhou, China, in 2013 and 2017, respectively.

He is currently an Associate Professor with the School of Mechanical and Electrical Engineering, Guangzhou University, Guangzhou. His research interests include adaptive and learning control, flexible mechanical systems, and robotics.

Chunliang Zhang received the B.Eng. and M.Eng. degrees from Xi'an Jiaotong University, Xi'an, China, in 1984 and 1987, respectively, and the Ph.D. degree from Zhejiang University, Hangzhou, China, in 2004.

He is currently a Professor with the School of Mechanical and Electrical Engineering, Guangzhou University, Guangzhou, China. His research interests include vibration control, manufacturing process automation, conditional monitor and fault diagnosis, CNC technology, and intelligent robot.

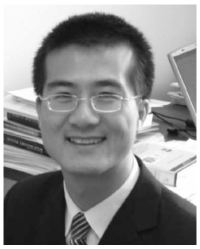

Qinmin Yang (Senior Member, IEEE) received the bachelor's degree in electrical engineering from the Civil Aviation University of China, Tianjin, China, in 2001, the Master of Science degree in control science and engineering from the Institute of Automation, Chinese Academy of Sciences, Beijing, China, in 2004, and the Ph.D. degree in electrical engineering from the University of Missouri–Rolla, Rolla, MO, USA, in 2007.

From 2007 to 2008, he was a Postdoctoral Research Associate with the University of Missouri–Rolla. From 2008 to 2009, he was a System Engineer with Caterpillar Inc., Deerfield, IL, USA. From 2009 to 2010, he was a Postdoctoral Research Associate with the University of Connecticut, Mansfield, CT, USA. Since 2010, he has been with the State Key Laboratory of Industrial Control Technology, College of Control Science and Engineering, Zhejiang University, Hangzhou, China, where he is currently a Professor. He has also held visiting positions with the University of Toronto, Toronto, ON, Canada, and Lehigh University, Bethlehem, PA, USA. His research interests include intelligent control, renewable energy systems, smart grid, and industrial big data.

He has been serving as an Associate Editor for the IEEE TRANSACTIONS ON SYSTEMS, MAN, AND CYBERNETICS: SYSTEMS, the *Transactions of the Institute of Measurement and Control*, and the IEEE/CAA JOURNAL OF AUTOMATICA SINICA.

Keum-Shik Hong (Fellow, IEEE) received the B.S. degree in mechanical design and production engineering from Seoul National University, Seoul, South Korea, in 1979, the M.S. degree in mechanical engineering from Columbia University, New York, NY, USA, in 1987, and the M.S. degree in applied mathematics and the Ph.D. degree in mechanical engineering from the University of Illinois at Urbana–Champaign, Champaign, IL, USA, in 1991.

In 1993, he joined the School of Mechanical Engineering, Pusan National University (PNU), Busan, South Korea. His Integrated Dynamics and Control Engineering Laboratory was designated a National Research Laboratory by the Ministry of Science and Technology of Korea in 2003. In 2009, under the auspices of the World Class University Program of the Ministry of Education, Science and Technology of Korea, he established the Department of Cogno-Mechatronics Engineering, PNU. His current research interests include brain–computer interface, nonlinear systems theory, adaptive control, distributed parameter systems, autonomous vehicles, and innovative control applications in brain engineering.

Dr. Hong has received many awards, including the Best Paper Award from the KFSTS of Korea in 1999, the F. Harashima Mechatronics Award in 2003, the IJCAS Scientific Activity Award in 2004, the Automatica Certificate of Outstanding Service in 2006, the Presidential Award of Korea in 2007, the ICROS Achievement Award in 2009, the IJCAS Contribution Award in 2010, the Premier Professor Award in 2011, the JMST Contribution Award in 2011, the IJCAS Contribution Award in 2011, and the IEEE Academic Award of ICROS in 2016. He served as an Associate Editor for *Automatica* from 2000 to 2006, and as the Editor-in-Chief for the *Journal of Mechanical Science and Technology* from 2008 to 2011, and is serving as the Editor-in-Chief for the *International Journal of Control, Automation, and Systems*. He was a past President of the Institute of Control, Robotics and Systems (ICROS), South Korea, and is the President-Elect of the Asian Control Association. He was the Organizing Chair of the ICROS-SICE International Joint Conference 2009, Fukuoka, Japan. He is a Fellow of the Korean Academy of Science and Technology, an ICROS Fellow, a member of the National Academy of Engineering of Korea, and many other societies.